JOURNAL OF RENEWABLE ENERGY AND SMART GRID TECHNOLOGY

Vol. 21, No. 2, July-December 2026



Metaheuristic Optimization of Multi-PV Placement in Distribution Networks with Dynamic Load Profiles

Siti Salwa Mat Isa[1*], Mohammad Nizam Ibrahim[1], Anuar Mohamad @ Ahmad[1], Shahilah Nordin[1], Nofri Yenita Dahlan [2], Hanis Farhah Jamahori[3]

[1]Faculty of Electrical Engineering, Universiti Teknologi MARA Cawangan Pulau Pinang, Permatang Pauh Campus, 13500 Seberang Prai, Pulau Pinang, Malaysia

[2]Solar Research Institute (SRI), Universiti Teknologi MARA, 40450 Shah Alam, Selangor, Malaysia

[3]Electrical and Electronics Department, Faculty of Engineering, Universiti Teknologi Petronas, 32610 Seri Iskandar, Perak, Malaysia

***Corresponding author's email**: salwaisa@uitm.edu.my

Article info:

Received: 26 December 2025
Revised: 6 August 2026
Accepted: 18 September 2026
DOI:
10.69650/rast.2026.265438

Keywords:

Photovoltaic (PV)
Metaheuristic Optimization
Coyote Optimization Algorithm
Time-Varying Load
Power Loss

ABSTRACT

The strategic integration of photovoltaic (PV) systems in distribution networks is essential for reducing power losses and enhancing voltage stability. However, traditional planning approaches often neglect the dynamic nature of daily load variations, leading to suboptimal PV deployments. This study addresses this gap by proposing a time-varying, load-sensitive optimization framework for multi-PV placement and sizing in the IEEE 33-bus radial distribution system. The objective is to minimize 24-hour active power losses across industrial, residential, and commercial load scenarios. A voltage-dependent load model and empirical PV generation data are integrated into the load flow analysis. The Coyote Optimization Algorithm (COA) is employed to solve a mixed-integer nonlinear programming (MINLP) problem, which involves both discrete variables (PV bus locations) and continuous variables (PV sizes), governed by nonlinear power flow constraints. The performance of COA is benchmarked against Particle Swarm Optimization (PSO) and Genetic Algorithm (GA). COA achieved the lowest active power loss in all cases. Under commercial loading, three PV units reduced active power loss by 38.48% relative to the base case and improved the voltage profile. In this scenario, Wilcoxon signed-rank tests found significant differences between COA and both PSO and GA over 30 runs. These findings underscore the importance of realistic load modelling and advanced optimization in planning resilient, high-performance PV deployments. The proposed methodology provides a realistic and statistically validated framework for PV planning studies involving distributed renewable generation.

1. Introduction

The global energy sector is experiencing rapid transformation, largely driven by the integration of distributed renewable energy resources (DERs), particularly photovoltaic (PV) systems, into distribution networks [1]. As a cornerstone of sustainable energy transition, PV deployment not only enables decentralized power generation and reduces greenhouse gas emissions [2, 3], but also minimizes network losses, enhances voltage profiles, and defers costly infrastructure upgrades [4, 5]. Rising electricity demand, the urgency to mitigate climate change, and strong policy commitments to decarbonization have further accelerated DER adoption across multiple levels of the power grid. Among these resources, PV systems stand out due to their scalability, declining installation costs, and ability to supply clean electricity directly to end-users.

Despite these advantages, large-scale PV integration introduces several operational challenges that must be carefully managed to ensure reliable and efficient network performance. The most pressing concern is the intermittency of solar energy, as PV output is inherently weather-dependent, leading to fluctuations that may result in power imbalances, voltage instability, and reverse power flows in radial distribution networks [6]. These challenges are further compounded by the time-varying nature of demand across industrial, residential, and commercial sectors. To address these issues, optimal planning of PV placement and sizing has emerged as a critical research focus. Strategic allocation of PV units can reduce active and reactive power losses, improve bus voltage profiles, and defer costly grid reinforcements, thereby enhancing system reliability and resilience [7, 8]. Conversely, poorly planned deployment may result in voltage violations, reverse power flows, and underutilization of generation capacity [9].

In parallel, metaheuristic algorithms have emerged as powerful tools for distributed generation (DG) planning, particularly in determining the optimal placement and sizing of PV units. Techniques such as Genetic Algorithm (GA), Particle Swarm Optimization (PSO), and the Coyote Optimization Algorithm (COA) are widely employed because they mimic natural or social behaviours to efficiently explore solution spaces while avoiding premature convergence. Unlike classical optimization methods, which become computationally prohibitive as system complexity increases, metaheuristics can effectively address large-scale, nonlinear, and multi-objective problems. This makes them particularly well suited

for distribution networks, where PV integration must balance technical efficiency, economic feasibility, and environmental sustainability.

A wide range of metaheuristics has been applied in PV planning, including GA, PSO, and more recent nature-inspired methods such as Crow Search, Black Widow, and Wild Horse optimizers [3, 5]. While many of these techniques have shown success, their performance often depends heavily on parameter tuning, and they may suffer from premature convergence or excessive computational burden. Since PV planning is inherently a mixed-integer nonlinear programming (MINLP) problem characterized by non-convexity and multiple operational constraints, robust algorithms are essential. In this context, COA has gained increasing attention due to its strong search dynamics, competitive convergence behaviour, and reduced parameter dependency [10].

Recent studies have employed diverse optimization frameworks for DG allocation. For instance, [11] developed a hybrid data-driven approach for reconfiguration and DG placement, while [12] addressed simultaneous allocation of DG units and shunt capacitors under high nonlinear load penetration. Similarly, [13] applied a Markov Decision Process (MDP) for network reconfiguration, and [14] proposed a Gaussian process learning-based voltage control strategy. In addition, [15] emphasized the role of load modelling by comparing voltage-dependent and constant load assumptions.

Although these contributions represent significant progress, most works continue to rely on simplified or static load assumptions, which fail to capture the dynamic variability of electricity demand. Traditional distribution planning approaches often assume constant or average demand levels for computational convenience, but in reality, load profiles vary considerably throughout the day due to consumer behaviour, operational cycles, and environmental conditions. Recent investigations [16, 17] have shown that disregarding such temporal variations can result in misaligned PV sizing and inappropriate site selection, thereby undermining the effectiveness of DG allocation. To address this issue, optimization frameworks incorporating time-varying load characteristics have been proposed to better align generation with actual demand patterns.

These approaches have demonstrated improvements in power loss reduction, voltage regulation, and overall system performance. For instance, [18] presented a hierarchical optimization model that accounts for time-dependent loads and generation, successfully mitigating phase imbalance in active distribution systems. Furthermore, [19, 20] investigated DG allocation under time-varying generation and load conditions, demonstrating the advantages of incorporating temporal demand characteristics into planning. In addition, recent works have emphasized the role of uncertainty-aware optimization frameworks. For example, [21] applied a PSO-based fuzzy max–min approach to microgrid planning with diverse load models, showing that constant power assumptions increase costs and losses while impedance-based models improve loading capability.

Similarly, [22] introduced a Modified Ant Lion Optimizer (MALO) to jointly integrate PV-DG and DSTATCOM under uncertain load and irradiance, achieving significant cost savings and voltage stability improvements in large-scale networks. Extending this direction, [23] proposed a Teaching–Learning Artificial Bee Colony (TLABC) algorithm for simultaneous PV and battery storage planning across a 24-hour horizon, outperforming GA and DE in loss reduction while accounting for generation and demand fluctuations. More recently, [24] developed a reinforcement learning-based Equilibrium Optimizer (RLEO) to optimize PV and BES deployment in residential, commercial, and industrial networks, reporting substantial improvements in both power loss reduction and system reliability. Collectively, these findings reinforce the importance of incorporating time-varying and uncertainty-driven characteristics into PV planning methodologies to ensure robust, practical, and scalable solutions.

In addition to these optimization frameworks, other studies have explored alternative approaches to distributed generation planning and renewable energy integration in power systems. For example, modified shuffled frog leaping algorithms have been applied for optimal distributed generation placement in radial distribution systems to enhance voltage stability and reduce network power losses [25]. Furthermore, hybrid renewable energy systems integrating solar and wind resources have been investigated to improve power quality and reliability in real-world grid applications [26]. These studies further highlight the growing importance of advanced optimization and renewable integration strategies in modern distribution network planning.

Building on this foundation, COA-based frameworks have been successfully applied to PV placement and sizing in distribution networks, with results consistently showing superior performance over GA, PSO, and Grey Wolf Optimizer (GWO) [27, 28]. Extending this line of research, the present study incorporates detailed 24-hour load profiles representing industrial, residential, and commercial sectors. This time-varying approach provides a more realistic and fine-grained modelling framework, ensuring that optimization outcomes align with actual consumption patterns and enabling a comprehensive evaluation of algorithmic performance under diverse load conditions.

Beyond technical optimization considerations, emerging smart grid applications increasingly rely on large volumes of operational data. Although the present study does not involve customer-level or privacy-sensitive data, secure data management is becoming increasingly important in modern smart grid environments. Future data-driven distribution network planning frameworks may benefit from privacy-preserving data processing and secure information exchange mechanisms to ensure reliable and trustworthy system operation.

While numerous studies have applied metaheuristic optimization techniques to photovoltaic placement and sizing problems, many continue to rely on constant load assumptions, simplified demand representations, or limited validation procedures. Although recent investigations have considered time-varying load conditions, uncertainty modelling, and renewable energy integration, the combined consideration of voltage-dependent sector-specific load behaviour, empirical photovoltaic generation data, multi-photovoltaic deployment, and statistical robustness assessment has received comparatively less attention in the literature despite its practical importance for realistic PV planning studies. Consequently, the influence of realistic demand dynamics on photovoltaic allocation strategies has not been extensively investigated.

The contribution of this study does not lie in proposing a new optimization algorithm. Instead, it lies in the development and validation of a sector-sensitive optimization framework that integrates voltage-dependent industrial, residential, and commercial load models with measured photovoltaic generation data. In addition, the framework incorporates systematic benchmarking, convergence analysis, and statistical evaluation through thirty independent

simulation runs and Wilcoxon signed-rank testing. This integrated approach provides a more realistic and rigorous assessment of photovoltaic allocation strategies under practical operating conditions and offers further insight into how load characteristics influence optimal photovoltaic placement and sizing in distribution networks. The main contributions are summarized as follows:

- Integration of voltage-dependent, time-varying sectoral load models in PV allocation analysis;
- Fair benchmarking of COA against PSO and GA under identical evaluation settings;
- Convergence and statistical performance assessment to evaluate robustness;
- Systematic evaluation of multi-PV integration impacts on power loss and voltage profile improvement.

2. Methodology

2.1 Test system

The IEEE 33-bus radial distribution system illustrated in Fig. 1 [27] is frequently used in distribution network research due to its realistic feeder layout and suitability for testing optimization algorithms. This system comprises 33 buses and 32 distribution lines, operates at a base voltage of 12.66 kV, and supports a total load of approximately 3.72 MW and 2.3 MVAR. The slack bus (Bus 1) is maintained at 1.02 p.u. to provide voltage reference across the system [29].

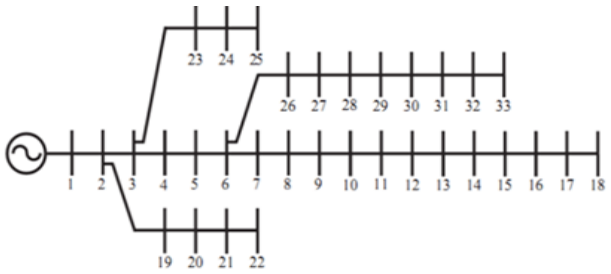

Fig. 1 IEEE 33-bus radial distribution network.

2.2 Load modelling

To represent actual load behavior, this study adopts dynamic daily demand profiles for three load categories: industrial, residential, and commercial. These are modelled using hourly normalized curves derived from empirical data and scaled to match the base load values.

Voltage sensitivity is incorporated using a voltage-dependent model [30]:

$$P_{load,i}(t) = P_{i,base}(t) \times V_i(t)^{\propto} \quad (1)$$

$$Q_{load,i}(t) = Q_{i,base}(t) \times V_i(t)^{\beta} \quad (2)$$

Here, $P_{load,i}(t)$ and $Q_{load,i}(t)$ denote the voltage-adjusted real and reactive loads at bus i and hour t, while $P_{i,base}(t)$ and $Q_{i,base}(t)$ represent the corresponding base load values. $V_i(t)$ is the voltage magnitude at bus i and time t. The parameters α and β represent the active and reactive power voltage sensitivity coefficients, respectively, which describe how real and reactive power demands at each bus vary in response to voltage changes. These coefficients are assigned based on load type, reflecting the distinct voltage dependency characteristics of industrial, residential, and commercial loads.

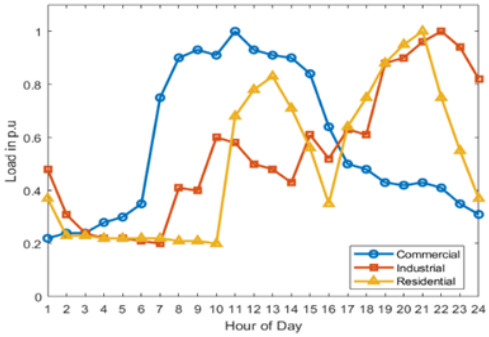

Fig. 2 Time-varying load demand profiles.

The adopted values are: industrial ($\alpha = 0.18$, $\beta = 6.00$), residential ($\alpha = 0.92$, $\beta = 4.04$), and commercial ($\alpha = 1.51$, $\beta = 3.40$) [30]. This formulation integrates voltage-dependent behavior into the load flow.

Fig. 2 [28] presents the normalized daily load curves that highlight the distinctive characteristics of commercial, residential, and industrial sectors. The commercial demand profile rises sharply during morning business hours, reaches its peak in the early afternoon, and gradually declines toward evening. This behavior reflects the operational schedules of offices, retail spaces, and service industries, where electricity use is concentrated within standard working hours.

In contrast, residential demand exhibits a dual-peak pattern driven by household activities. A moderate rise is observed in the morning, corresponding to breakfast preparation and early domestic appliance use, while the more dominant peak occurs in the evening as families return home, resulting in increased usage of lighting, cooking, cooling, and entertainment devices. This evening dominance makes the residential profile particularly relevant when considering PV integration, as solar output typically diminishes at this time, leading to a mismatch between supply and demand.

The industrial demand profile follows a more gradual but sustained trajectory. Loads increase steadily during the day, reflecting continuous production processes and machinery operation, and often peak late at night due to shift-based or 24-hour industrial activities. Unlike commercial and residential loads, industrial demand is less correlated with daylight availability, making it a significant contributor to base load in the distribution system.

These distinctions underscore the importance of sector-specific load modeling in PV integration studies. If a constant or averaged load curve were assumed, the unique temporal characteristics of each sector would be masked, potentially leading to suboptimal PV placement and sizing decisions. By explicitly accounting for commercial, residential, and industrial demand variations, the present study ensures that the optimization framework reflects real-world operating conditions and captures the interaction between PV generation and load dynamics across different sectors.

2.3 PV generation data

The PV generation dataset was obtained through a meter logging system established and maintained by the Solar Research Institute (SRI), Universiti Teknologi MARA (UiTM). The dataset covers the period from May to December 2023 and consists of 30-minute interval power output measurements from eleven grid-connected PV systems installed on campus buildings. Since the measurements were collected over several months, the raw data inherently capture variations caused by irradiance fluctuations, weather conditions, and seasonal changes.

To develop a representative input for the optimization framework, the raw measurements were processed and averaged into hourly values, yielding a 24-hour PV generation profile used as the PV generation input for the optimization model. The averaging process was adopted to derive a representative daily profile while preserving the seasonal and weather-related variability embedded within the original measurement dataset.

In the simulation model, each PV unit is represented as a Type-I distributed generator, supplying only active power to the distribution network. Reactive power injection is excluded, reflecting the typical operating characteristics of grid-connected PV inverters. The reference output profile corresponds to the measured generation from a single PV panel, which is then scaled according to the number of panels determined by the optimization algorithm for each scenario. Consequently, the magnitude of PV output varies with load type and penetration level, while the temporal profile maintains a consistent shape.

Fig. 3 illustrates the empirical hourly PV generation curve derived from the UiTM dataset. The profile follows a bell-shaped distribution typical of tropical conditions, with negligible output before 7:00 a.m. and after 7:00 p.m., a rapid increase between 8:00 a.m. and 11:00 a.m., and a peak of approximately 3.6 kW between 12:00 p.m. and 2:00 p.m. Thereafter, output gradually declines toward the evening. This realistic shape reflects the strong midday irradiance and sharp morning/evening transitions observed in Malaysia's equatorial climate.

The use of empirical data ensures that the simulations reflect realistic operating conditions rather than synthetic assumptions. The dataset inherently captures fluctuations caused by local weather and irradiance variability, thereby enhancing the representativeness of the results. Notably, this dataset has been previously validated in [31] for distribution network optimization, further reinforcing its reliability.

Beyond providing a baseline PV shape, the profile emphasizes the inherent intermittency and temporal concentration of solar power. During peak hours, generation may surpass local demand, while during off-peak hours (early morning and late evening), PV contribution is minimal. These mismatches highlight the need for strategic PV allocation in distribution networks, particularly under time-varying industrial, residential, and commercial loads. By embedding this empirical curve into the optimization process, the study ensures that the outcomes reflect both the opportunities and challenges of real-world PV deployment.

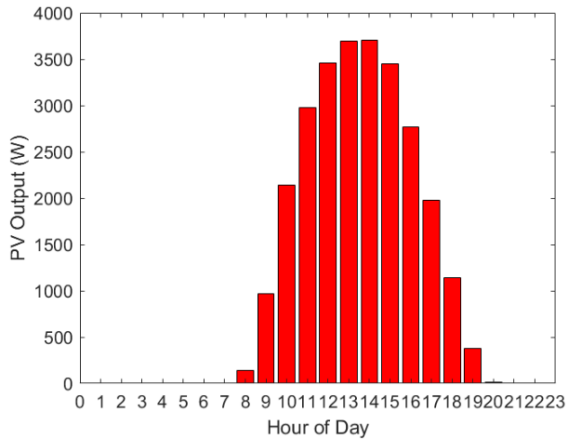

Fig. 3 Average hourly PV generation profile based on measured daily output.

2.4 PV integration in load flow analysis

The PV systems in this study are modelled as Type I distributed generation units, represented as negative power loads that inject only real power into the distribution network. Each PV system operates at unity power factor, which implies no reactive power contribution ($Q_{PV}=0$). When installed at a particular bus, the PV output reduces the net active power demand at that location, while the reactive load remains unchanged. This decrease in current flow results in lower power losses along upstream branches. Although modern PV inverters are capable of providing reactive power support for voltage regulation, this capability is not considered in the present framework in order to focus on evaluating the impact of active power allocation on power loss reduction under time-varying load conditions.

The active and reactive power losses across a branch i after PV integration can be calculated using the following expressions [32, 33]:

$$P_{loss,i}^{PV} = R_i \frac{(P_{k+1} - P_{PV})^2 + Q_{k+1}^2}{V_{k+1}^2} \quad (3)$$

$$Q_{loss,i}^{PV} = X_i \frac{(P_{k+1} - P_{PV})^2 + Q_{k+1}^2}{V_{k+1}^2} \quad (4)$$

In the above expressions, R_i and X_i represent the resistance and reactance of branch i, respectively; P_{k+1} and Q_{k+1} denote the original real and reactive power demands at the receiving bus $k+1$; P_{PV} is the photovoltaic generation output at that bus during hour t; and V_{k+1} is the voltage magnitude at bus $k+1$. These equations reflect the reduction in system losses due to the active power support provided by PV units, which becomes particularly significant under time-varying load and generation conditions. Recent works have demonstrated the effectiveness of such formulations in quantifying loss reduction from distributed PV integration [3].

2.5 Objective function

The primary objective of this study is to minimize the total real power losses in the IEEE 33-bus distribution system over a 24-hour period. Power loss minimization enhances system efficiency, reduces energy wastage, and improves overall operational performance in distribution networks. Given the integration of distributed PV systems under time-varying load conditions, this objective becomes more critical as both generation and demand fluctuate throughout the day. The total active power loss at each hour is calculated and summed across the 24-hour horizon. The mathematical formulation of the objective function is given as [24].

$$min \sum_{i=1}^{24} (P_{Loss,t}) \quad (5)$$

Where $P_{loss}(t)$ represents the total real power loss of the distribution network at hour, t. This optimization is subject to several system and operational constraints related to PV placement, size limits, and voltage boundaries, which are described in the following subsections.

2.5.1 PV location and size constraints

The installation of PV systems is restricted to load buses, excluding the slack bus, to ensure effective local energy support. Mathematically, the allowable range for the PV installation bus is [30]:

$$2 \leq PV_{bus} \leq N_{bus} \quad (6)$$

Here, PV_{bus} denotes the bus at which the PV system is installed, and N_{bus} is the total number of buses in the system. Additionally,

the installed PV capacity must not exceed the total real power demand of the network. This constraint is expressed as [30]

$$0 \leq PV_{size} \leq \sum_{i=1}^{N_{bus}} P_{i,base} \quad (7)$$

In this expression, PV_{size} represents the installed capacity of the PV system, and $P_{i,base}$ is the real power demand at bus *i*.

2.5.2 Voltage constraint

$$0.95 \leq V_i \leq 1.02\ p.u \quad (8)$$

This voltage limit formulation is widely adopted in PV allocation studies within distribution networks and has been validated in standard test systems. During the optimization process, candidate solutions that violate the voltage constraint ($0.95 \leq V_i \leq 1.02$ p.u.) are penalized or rejected to ensure that all feasible solutions maintain acceptable voltage levels across the distribution network. In this study, the optimization framework focuses on fundamental network constraints including power balance and voltage limits to evaluate the technical impact of PV allocation. More advanced operational constraints such as reactive power capability, reverse power flow limits, and line thermal limits are not explicitly modelled and remain important considerations for future research.

2.6 Optimization approach: Coyote Optimization Algorithm (COA)

The COA is a nature-inspired metaheuristic that simulates the social behavior and adaptability of coyotes living in packs [34]. Unlike traditional optimization methods that rely heavily on mathematical gradients or convex assumptions, COA explores the search space through cooperative and competitive interactions within and between coyote packs. This mechanism enables the algorithm to efficiently navigate complex, nonlinear, and multi-modal search problems, which are typical in power system planning.

In the present study, COA is employed to identify the optimal locations and penetration levels of one, two, or three PV systems in a radial distribution network. The primary objective is to minimize total active power losses while ensuring bus voltages remain within the prescribed operational limits. Each solution candidate, or "coyote," encodes a set of decision variables representing PV capacities (in kW) and their associated bus locations.

The fitness of each candidate solution is determined using 24-hour load flow simulations that incorporate both voltage-dependent load models and empirical PV output profiles. By embedding sector-specific demand variations into the fitness evaluation, the optimization process ensures that the resulting PV configurations are not only technically feasible but also resilient to daily fluctuations in load.

The optimization begins with the initialization of a population of coyotes distributed across several packs. Each coyote is randomly assigned PV sizes and bus locations within specified lower and upper bounds. In each iteration, coyotes update their positions based on two key influences: the alpha coyote of the pack, representing the current best-performing solution, and the social tendency, which captures the collective direction of the pack. This dual influence allows COA to balance exploration (searching new areas of the solution space) and exploitation (refining promising regions).

A crucial feature of COA is the birth and death mechanism, which introduces new "pups" into the population. If a newly generated coyote (pup) achieves better fitness than the worst-performing member of the pack, it replaces the latter. This evolutionary strategy maintains population diversity, reduces the likelihood of premature convergence, and strengthens the algorithm's global search capability. Such diversity preservation is especially important in PV planning, where the solution space is highly nonlinear due to the interaction between load variability, voltage constraints, and distributed generation placement [35, 36].

The optimization continues until the stopping criterion is met. In this study, the termination condition is defined by the maximum number of function evaluations (N_{feval} = 15,000), which provides a balance between computational efficiency and solution accuracy. Once this limit is reached, the best-performing coyote is selected as the final solution, representing the optimal configuration of PV locations and penetration levels. The algorithm thus outputs a deployment plan that minimizes active power losses and enhances voltage stability across the network.

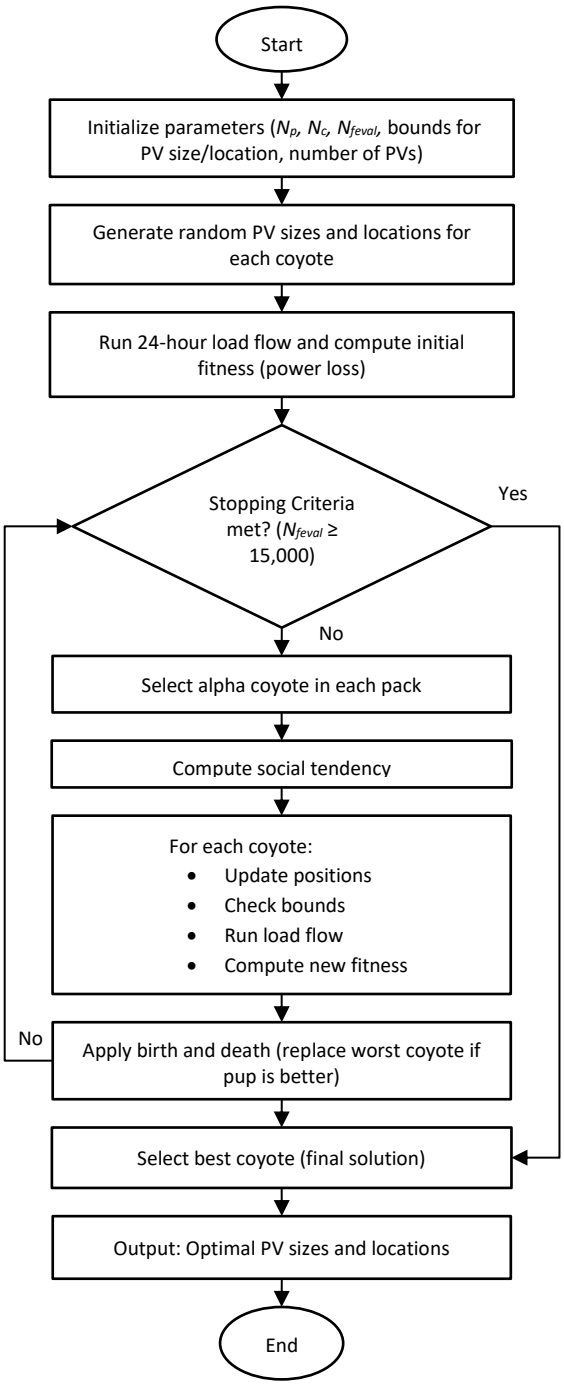

Fig. 4 Flowchart of the COA process for optimizing PV location and size with power loss reduction.

Fig. 4 illustrates the complete workflow of the COA implementation. The process begins with initialization, followed by iterative evaluation of pack dynamics, alpha selection, position updates, and the application of the birth–death mechanism. This iterative cycle continues until until the function evaluation limit is reached, at which point the best coyote is chosen as the optimal solution. By integrating real PV generation data, time-varying demand patterns, and evolutionary optimization, the proposed COA framework overcomes the limitations of static or deterministic methods and offers a scalable, practical planning tool for modern distribution systems [37].

This comprehensive optimization approach integrates real-world PV generation data, time-dependent load modeling, and evolutionary computation to address the critical limitations identified in prior literature. By aligning PV deployment with actual consumption patterns and system constraints, the proposed COA framework supports accurate, scalable, and practical planning for future distribution networks.

2.7 Benchmark algorithms for comparison

To evaluate the effectiveness of the proposed COA-based optimization, two widely used metaheuristic algorithms, PSO and GA, were implemented for benchmarking purposes. These algorithms were selected due to their established success, simplicity, and frequent application in power system optimization, particularly in PV sizing and placement studies. Their inclusion allows a consistent and transparent comparison framework for evaluating the performance of COA under identical optimization conditions. PSO mimics the collective behaviour of particles navigating a solution space, while GA emulates evolutionary processes through selection, crossover, and mutation [38].

To ensure transparency and reproducibility, the key parameter settings for all optimization algorithms are clearly specified. For the COA, the number of decision variables was set to six, with lower and upper bounds defined according to the PV sizing and bus location limits. The algorithm was configured with 10 coyote packs and 5 coyotes per pack, resulting in a total population of 50. The stopping criterion was set to a maximum of 15,000 function evaluations.

For PSO, the population size was also set to 50, with six decision variables. The inertia weight was initialized at w=1.0 and reduced by a damping factor $wdamp$=0.99 at each iteration. The acceleration coefficients were set to $c1$=1.5 and $c2$=2.0, and velocity limits were defined as ±10% of the decision variable range. To match the COA's evaluation budget, the number of iterations was set to 300, resulting in 15,000 function evaluations. For GA, the population size was 50, with six decision variables. Standard genetic operations were applied, and the number of generations was also set to 300 to align with the same function evaluation count of 15,000.

All algorithms were executed under consistent problem dimensionality and stopping criteria to ensure a fair and balanced performance comparison. Although PSO and GA were not the primary focus of this study, their inclusion provides a comparative perspective on the performance, robustness, and consistency of the COA approach in solving the PV placement and sizing problem.

2.8 Simulation setup

All simulations are conducted in MATLAB R2023b. Each test scenario combines a specific load type (industrial, residential, or commercial) with varying numbers of PV systems (1, 2, and 3). Performance metrics include total real power loss, reactive power loss, PV penetration level, and computational time. To assess algorithmic robustness, thirty independent trials are conducted for each case, and the statistical results are reported.

Although the present study focuses on the IEEE 33-bus system, the proposed optimization framework is general and can be extended to larger distribution networks without modification to the underlying optimization methodology. Consequently, the framework remains applicable to more complex distribution systems, subject to the availability of appropriate network and load data.

3. Results and discussion

This section presents and analyzes the simulation outcomes for optimal PV placement and sizing using the COA, with comparisons to PSO and GA. The analysis addresses total power loss, voltage profiles, convergence behavior, and statistical performance across industrial, residential, and commercial load categories. The effect of increasing the number of PV systems (from one to three) is evaluated to demonstrate the role of distributed generation in enhancing system reliability, efficiency, and voltage stability. Results are structured around simulation outcomes, voltage improvements, convergence performance, and statistical consistency, thereby providing a comprehensive performance assessment of the algorithms under time-varying load conditions.

Table 1 PV integration results under time-varying load scenarios.

Load type	Method	PV Location	PV Size [MW]	Ploss (PV) [kW]	Ploss (Base) [kW]	Ploss Reduction [%]	Qloss (PV) [kVAR]	Qloss (Base) [kVAR]	Qloss Reduction [%]	PV Penetration [%]	Comp. Time [s]
Industrial	COA	6	1.57	1319.68	1516.94	13	907.16	1025.36	11.53	23.62	131.89
	PSO	6	1.55	1320.46		12.95	907.17		11.53	23.64	227.65
	GA	6	1.56	1319.7		13	907.17		11.53	23.45	227.65
Residential	COA	6	1.79	1119.33	1374.39	18.56	775.93	928.33	16.42	29.18	182.09
	PSO	6	1.76	1120.51		18.47	776.45		16.36	29.12	122.61
	GA	6	1.77	1119.53		18.54	776.18		16.39	28.89	237.38
Commercial	COA	6	2.37	1189.74	1631.01	27.06	838.88	1100.82	23.8	34.35	172.92
	PSO	6	2.36	1191.16		26.97	839.37		23.75	34.14	156.13
	GA	6	2.37	1189.75		27.05	838.85		23.8	34.26	314.66

Table 2 PV integration results under time-varying load scenarios.

Load type	Method	PV Location	PV Size [MW]	Ploss (PV) [kW]	Ploss (Base) [kW]	Ploss Reduction [%]	Qloss (PV) [kVAR]	Qloss (Base) [kVAR]	Qloss Reduction [%]	PV Penetration [%]	Comp. Time [s]
Industrial	COA	13	0.53	1272.82	1516.94	16.09	861.52	1025.36	15.98	23.25	479.31
		29	0.73								
	PSO	13	0.52	1275.37		15.92	869.08		15.24	23.54	453.03
		29	0.75								
	GA	13	0.53	1273.46		16.05	861.59		15.97	23.53	460.13
		29	0.73								
Residential	COA	13	0.62	1057.76	1374.39	23.04	716.06	928.33	22.87	29.92	446.55
		30	0.79								
	PSO	13	0.62	1062.93		22.66	726.19		21.77	29.31	392
		30	0.78								
	GA	13	0.62	1058.64		22.97	716.15		22.86	30.11	413.94
		30	0.8								
Commercial	COA	13	0.8	1082.37	1631.01	33.64	734.39	1100.82	33.29	39.07	445.54
		29	1.14								
	PSO	13	0.82	1085.18		33.47	741.11		32.68	39.95	582.12
		29	1.15								
	GA	13	0.81	1085.1		33.47	741.11		32.68	39.36	503.37
		30	1.14								

Table 3 PV integration results under time-varying load scenarios.

Load type	Method	PV Location	PV Size [MW]	Ploss (PV) [kW]	Ploss (Base) [kW]	Ploss Reduction [%]	Qloss (PV) [kVAR]	Qloss (Base) [kVAR]	Qloss Reduction [%]	PV Penetration [%]	Comp. Time [s]
Industrial	COA	13	0.51	1239.36	1516.94	18.3	840.7	1025.36	18.01	27.48	175.71
		24	0.72								
		30	0.6								
	PSO	14	0.49	1248.95		17.67	849.54		17.15	27.52	463.03
		24	0.71								
		30	0.63								
	GA	14	0.49	1244.62		17.95	845.86		17.51	27.69	341.57
		24	0.72								
		30	0.64								
Residential	COA	14	0.5	1014.87	1374.39	26.16	690.36	928.33	25.63	35.46	166.46
		24	0.85								
		30	0.82								
	PSO	14	0.58	1023.49		25.53	696.82		24.94	34.83	463.55
		24	0.83								
		30	0.73								
	GA	14	0.56	1018.25		25.91	692.26		25.43	34.26	482.68
		24	0.8								
		30	0.74								
Commercial	COA	14	0.73	1003.4	1631.01	38.48	683.6	1100.82	37.9	41.99	117.66
		24	1.17								
		30	1								
	PSO	13	0.95	1013.69		37.95	692.75		37.07	41	550.21
		24	0.99								
		30	0.95								
	GA	13	0.95	1014.04		37.83	693.55		37	41.03	331.07
		24	0.99								
		30	0.89								

3.1 Simulation results

Tables 1–3 present the optimization results for single, dual, and triple PV integration under industrial, residential, and commercial load scenarios using the COA, PSO, and GA algorithms. The results evaluate the influence of PV deployment on key performance indicators including active power loss (Ploss), reactive power loss (Qloss), PV penetration level, and computational time. Table 1 summarizes the results for single PV integration. Across all load scenarios, the optimization algorithms consistently identify Bus 6 as the optimal installation location, indicating that this bus provides the most effective position for minimizing feeder losses. The introduction of a single PV unit leads to noticeable reductions in both active and reactive power losses.

For the industrial load case, the base-case active power loss of 1516.94 kW is reduced to approximately 1319.68 kW, corresponding to a reduction of about 13%. For residential loads, the loss decreases from 1374.39 kW to 1119.33 kW, representing a reduction of 18.56%. The most significant improvement occurs under the commercial load scenario, where active power loss decreases from 1631.01 kW to 1189.74 kW, achieving a 27.06% reduction. Although all algorithms identify similar installation locations and PV capacities, COA generally achieves slightly lower loss values and higher PV penetration levels. PSO demonstrates the shortest computational time, while GA produces comparable technical results with moderate computational effort.

Table 2 presents the results for dual PV integration, where the addition of a second PV unit further enhances system performance. In this case, the optimal deployment locations are typically identified at Buses 13 and 29 or Buses 13 and 30, depending on the load scenario and optimization method. With two PV units installed, reductions in active power loss become more pronounced. For the industrial load case, the loss decreases to approximately 1272.82 kW, corresponding to a 16.09% reduction. Residential loads achieve a reduction of approximately 23.04%, while the commercial load scenario records the highest improvement, reaching 33.64% reduction in active power loss using COA. Reactive power losses exhibit similar improvements, while PV penetration levels increase significantly, reaching approximately 39% in the commercial scenario.

Further improvements are observed with triple PV integration, as shown in Table 3. In this configuration, the optimal PV locations are distributed across the mid and downstream sections of the feeder. For the commercial load case, COA identifies Buses 14, 24, and 30, while PSO and GA select Buses 13, 24, and 30, indicating that the algorithms consistently allocate PV units along electrically influential buses to maximize loss reduction. For industrial loads, the active power loss decreases to 1239.36 kW, representing an 18.30% reduction. Residential loads experience a reduction of 26.16%, while the commercial load case achieves the largest improvement, where the active power loss decreases to 1003.40 kW, corresponding to a 38.48% reduction. In this scenario, PV penetration exceeds 41%, indicating effective utilization of distributed renewable generation.

Fig. 5 illustrates the variation in total active power loss as the number of PV units increases from one to three under the three load categories. A consistent downward trend can be observed across all scenarios, demonstrating that additional PV installations effectively reduce feeder current and network losses by supplying power closer to load demand. Among the evaluated load types, the commercial load scenario exhibits the most pronounced reduction,

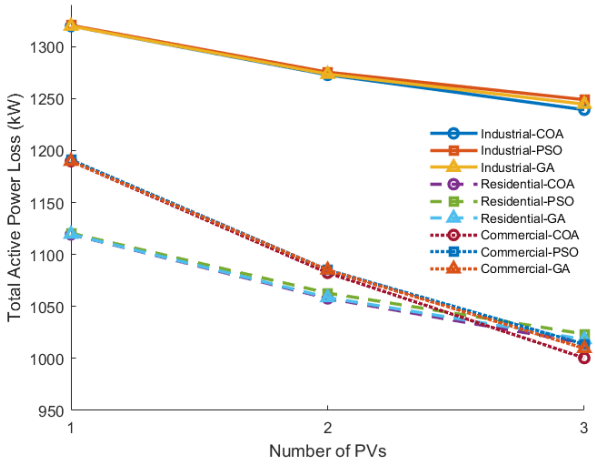

Fig. 5 Active power loss comparison across PV configurations (Ploss in kW).

decreasing from approximately 1189.74 kW with one PV to about 1003.40 kW with three PV units when optimized using COA. This stronger impact can be attributed to the alignment between daytime PV generation and commercial demand patterns, which allows PV output to directly offset a larger portion of feeder loading.

Industrial and residential loads exhibit similar trends, although the reductions are slightly more moderate. Industrial losses decrease from approximately 1319.68 kW to 1239.36 kW, while residential losses decline from 1119.33 kW to 1014.87 kW as the number of PV units increases. Across all PV configurations, COA achieves the lowest active power loss values, followed by GA and PSO, indicating its stronger search capability in identifying effective PV locations and sizes. These results demonstrate that progressive PV integration significantly enhances distribution network efficiency by reducing network losses under time-varying load conditions.

3.2 Voltage profile improvement

Fig. 6 illustrates the voltage profile across all buses for the commercial load scenario under four operating conditions: the base case (without PV) and cases with 1 PV, 2 PVs, and 3 PVs integrated using COA. For voltage profile analysis, the PV buses are maintained at 1.02 p.u. while assessing the impact of PV integration on voltage behavior throughout the feeder. This assumption is adopted solely for voltage profile evaluation and does not imply reactive power support from the PV system.

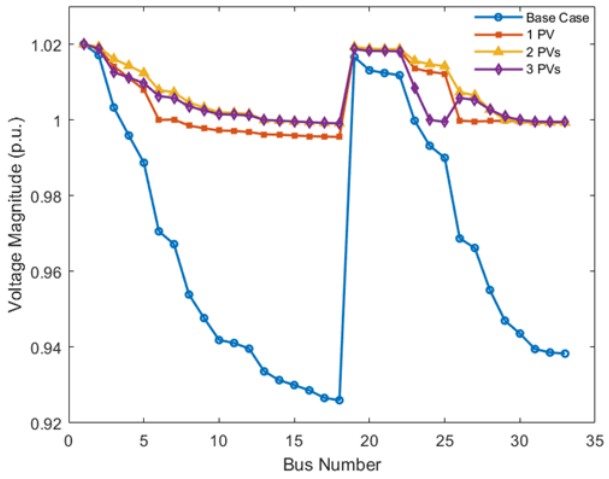

Fig. 6 Voltage profiles under commercial loading for the base case and configurations with one, two, and three PV units using COA.

In the base case, the voltage profile exhibits a pronounced decline along the feeder, particularly at downstream buses, with the minimum voltage falling below 0.93 p.u. This behavior reflects the significant voltage drop associated with high commercial loading conditions and the absence of local generation support. Following the installation of a single PV unit at Bus 6, a noticeable improvement in voltage magnitude is observed around the PV location. However, despite this localized enhancement, several downstream buses continue to experience voltage deterioration, indicating that a single PV installation provides only limited improvement to the overall feeder voltage profile.

The integration of two PV units at Buses 13 and 29 leads to a more substantial improvement in voltage performance. Voltage levels across mid-feeder and end-of-line buses increase closer to the nominal value of 1.0 p.u., resulting in a reduced depth of voltage drops and improved voltage stability. This improvement becomes even more pronounced when three PV units are installed at Buses 14, 24, and 30. Under this configuration, the voltage profile becomes considerably flatter and more uniform, with most buses operating within the range of 0.99 to 1.02 p.u., demonstrating effective voltage regulation across the entire feeder.

Beyond improving minimum voltage levels, the deployment of multiple PV systems significantly enhances voltage uniformity throughout the network. This effect is particularly important in radial distribution systems, where cumulative line impedance causes downstream buses to be more vulnerable to voltage degradation. The results clearly show that distributing PV units across electrically distant buses is more effective than concentrating capacity at a single location, as it mitigates localized voltage rise while extending voltage support deeper into the feeder.

From a practical planning perspective, these findings indicate that voltage regulation benefits scale nonlinearly with the number of PV installations. While a single PV mainly improves voltage conditions near its point of connection, multi-PV configurations provide system-wide reinforcement by mitigating both under-voltage conditions and excessive voltage gradients. This characteristic is especially valuable in networks with heterogeneous load profiles, where voltage sensitivity varies across industrial, residential, and commercial sectors.

Furthermore, maintaining PV bus voltages at 1.02 p.u. enables PV units to function as stabilizing anchors within the distribution network. By reducing reactive power flow requirements, these PV installations indirectly support adjacent buses and enhance overall voltage resilience under heavy loading conditions. Consequently, the results confirm that optimal PV planning should consider not only power loss minimization but also voltage sensitivity and feeder topology to ensure robust and reliable operation under dynamic load variations.

Overall, the voltage profile analysis reinforces the power loss reduction findings, demonstrating that strategically distributed PV deployment simultaneously enhances system efficiency and voltage stability. This dual benefit highlights the importance of coordinated PV placement and sizing in achieving resilient and high-performance distribution networks under time-varying load conditions.

3.3 Convergence behavior of optimization algorithms

Fig. 7 presents the convergence behavior of the three metaheuristic algorithms: COA, PSO, and GA, under the commercial load scenario with three PV integrations.

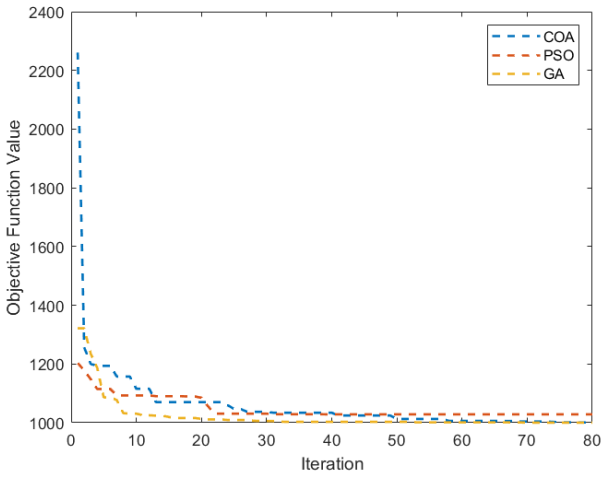

Fig. 7 Convergence behavior of COA, PSO, and GA for commercial load with three PVs.

This particular case was selected because it demonstrated the highest overall power loss reduction and voltage improvement among all tested scenarios, making it the most technically demanding and representative for evaluating algorithm performance. The COA algorithm begins with an initial objective value of approximately 2260.80 kW and quickly reduces it by nearly 50 percent within the early iterations. It then continues to improve steadily and ultimately converges to a final value of around 999.95 kW.

PSO starts at approximately 1203.75 kW and converges rapidly within the first 25 iterations. However, it settles at a higher loss value of about 1028.98 kW, indicating a tendency to fall into local minima. In comparison, GA starts at around 1321.40 kW and follows a more gradual decline, converging to approximately 1000.35 kW. This behavior reflects a balanced trade-off between convergence speed and solution accuracy.

A comparative assessment of these results highlights that COA achieves the lowest final objective value among the evaluated algorithms, demonstrating its superior capability in effectively exploring and exploiting the search space. While GA provides consistent and reliable performance with moderate convergence speed, PSO excels in computational efficiency but sacrifices solution quality. These observations collectively confirm the suitability of COA for addressing complex PV placement and sizing problems under dynamic, time-varying load conditions.

The observed convergence trends can be further explained by the inherent search mechanisms of each algorithm. COA leverages its pack-based social structure, where alpha guidance facilitates local refinement while social tendency and birth–death mechanisms promote global exploration. This balanced interaction enables COA to avoid premature convergence and maintain steady improvement throughout the optimization process. In comparison, PSO's aggressive velocity updates toward global and personal best positions lead to rapid early convergence but increase vulnerability to local minima in highly nonlinear solution spaces. GA relies on stochastic crossover and mutation operators, which preserve population diversity but require additional iterations to refine solutions. These fundamental differences in search dynamics account for the superior stability, robustness, and repeatability exhibited by COA in the statistical evaluations.

3.4 Statistical performance comparison of optimization algorithms

Table 4 presents the statistical results obtained from thirty independent simulation runs for each optimization algorithm under the 3-PV commercial load scenario. The table summarizes the best, mean, worst, and standard deviation values of the total active power loss achieved by COA, PSO, and GA. These statistical indicators provide a more comprehensive evaluation of the robustness, reliability, and repeatability of the optimization algorithms when applied to the PV placement problem.

The results indicate that COA demonstrates the most robust optimization performance among the evaluated algorithms. The best power loss achieved by COA is 999.83 kW, while the mean and worst values are 1003.40 kW and 1009.01 kW, respectively. Furthermore, COA exhibits the smallest standard deviation of 3.51 kW, indicating that the algorithm consistently converges to near-optimal solutions across repeated simulation runs. In comparison, PSO and GA show larger performance variations. Although both algorithms are capable of achieving competitive best-case solutions, their mean and worst values are considerably higher. PSO records a mean power loss of 1013.69 kW and a worst value of 1034.31 kW, with a standard deviation of 15.02 kW, indicating significant variability between runs. Similarly, GA produces a mean power loss of 1014.04 kW and a worst value of 1034.99 kW, with a standard deviation of 15.27 kW, suggesting less consistent convergence behaviour compared with COA.

To further evaluate the statistical significance of the performance differences among the algorithms, the Wilcoxon signed-rank test was performed based on the results of the thirty independent runs. The Wilcoxon test is a non-parametric statistical method commonly used to compare stochastic optimization algorithms without assuming normal distribution of the data. The pairwise comparison results are presented in Table 5.

The Wilcoxon signed-rank test results indicate that the performance differences between COA and both benchmark algorithms are statistically significant at the 5% significance level. Specifically, the comparison between COA and PSO yields a p-value of 0.0157, while the comparison between COA and GA produces a p-value of 0.0285. Since both values are below the significance threshold of 0.05, the null hypothesis of equal performance is rejected, confirming that COA achieves significantly lower power loss than both PSO and GA under the commercial load scenario with three PV units.

In contrast, the comparison between PSO and GA results in a p-value of 0.4528, indicating that the performance difference between these algorithms is not statistically significant. These findings demonstrate that COA not only achieves lower average power loss but also delivers statistically superior optimization performance compared with the benchmark methods.

Furthermore, COA exhibits the lowest standard deviation among the evaluated algorithms, indicating greater consistency and reduced variability across repeated simulation runs. Combined with its superior convergence behaviour, the statistical results confirm the robustness and effectiveness of COA for solving PV placement and sizing problems under time-varying load conditions. Overall, the analysis demonstrates that COA provides a more stable and reliable optimization framework, consistently producing high-quality solutions while maintaining superior performance compared with PSO and GA.

Table 4 Statistical results for power loss using COA, PSO and GA.

Method	Best Ploss (kW)	Mean Ploss (kW)	Worst Ploss (kW)	Std. Dev. (kW)
COA	999.83	1003.40	1009.01	3.51
PSO	999.84	1013.69	1034.31	15.02
GA	999.89	1014.04	1034.99	15.27

Table 5 Wilcoxon signed-rank test results.

Comparison	p-value	Significance (α = 0.05)
COA vs PSO	0.0157	Significant
COA vs GA	0.0285	Significant
PSO vs GA	0.4528	Not Significant

3.5 Summary of findings

The analysis across multiple scenarios confirms that distributed PV integration enhances both the technical efficiency and voltage stability of distribution networks under time-varying load conditions. As the number of PV units increases, power losses decrease progressively, while voltage profiles become more uniform due to improved power support along the feeder. The comparative evaluation of optimization algorithms indicates that although PSO and GA remain effective, COA consistently provides more stable and reliable solutions across repeated trials.

The results also highlight the important relationship between PV allocation and sector-specific load characteristics. Industrial loads, characterized by relatively steady demand patterns, demonstrate moderate but consistent improvements. Residential loads show intermediate loss reductions, while commercial loads show the greatest reduction due to stronger alignment between daytime demand and PV generation. These findings highlight the importance of incorporating sector-specific load characteristics in PV planning studies.

Overall, the results demonstrate that combining realistic load modelling with robust optimization techniques can significantly improve PV allocation strategies in distribution networks. These findings also provide a basis for future investigations involving economic considerations, energy storage integration, and large-scale distribution system applications, which are discussed further in the concluding section.

4. Conclusion

This paper proposed a Coyote Optimization Algorithm (COA)-based framework for the optimal placement and sizing of photovoltaic (PV) systems in distribution networks under realistic time-varying load conditions. The main objective was to minimize total active power losses while maintaining acceptable voltage levels across the IEEE 33-bus system. The proposed method incorporated empirical PV generation data and sector-specific, voltage-dependent load modeling to accurately reflect the dynamic behavior of industrial, residential, and commercial demand profiles over a 24-hour period.

Simulation results demonstrate that COA consistently achieves lower active and reactive power losses, improved voltage profiles, and more stable convergence behaviour compared with PSO and GA. The commercial load case with three PV units achieved the highest power loss reduction of 38.48%. In the commercial case with three PV units, COA exhibited the lowest standard deviation over 30 independent simulation runs. In addition, Wilcoxon signed-rank testing verified that the performance improvements achieved by COA are statistically significant when compared with both PSO and GA,

confirming its statistically superior optimization performance for the evaluated PV placement and sizing problem.

Beyond the numerical improvements, the findings provide valuable insights for distribution network planning by highlighting the importance of considering sector-specific load characteristics in PV allocation studies. The results demonstrate that optimal PV placement and sizing strategies are highly dependent on load behavior and should therefore be adapted to the distinct consumption patterns of industrial, residential, and commercial sectors. By incorporating realistic load dynamics and measured PV generation data, the proposed framework offers a more representative assessment of PV integration strategies and supports more informed planning decisions for modern distribution systems.

Nevertheless, this study has certain limitations. Economic considerations such as installation cost, maintenance, and variability in energy pricing were not included, which limits the current framework to a purely technical evaluation. Similarly, factors such as uncertainty in solar generation, demand forecasting errors, and real-time operational constraints were outside the scope of this work. In addition, the computational effort of the proposed optimization framework is influenced by the 24-hour time-varying simulation process, where each candidate solution requires repeated load flow calculations across all hourly operating conditions. Addressing these limitations in future work will provide a more comprehensive decision-making tool that integrates both technical and economic aspects of PV planning.

Future research should extend this framework to incorporate Battery Energy Storage Systems (BESS), enabling joint optimization of PV-BESS systems for load shifting, peak shaving, and improved grid flexibility. Expanding the framework into multi-objective optimization will allow simultaneous evaluation of technical and economic objectives, ensuring that power loss minimization is balanced against cost, reliability, and environmental considerations. In this context, economic performance metrics such as Net Present Value (NPV), Levelized Cost of Energy (LCOE), and payback period can be incorporated to support more comprehensive planning decisions for utility operators. In addition, future studies may explore hybrid optimization strategies or comparisons with additional state-of-the-art metaheuristic algorithms, such as JAYA, Grey Wolf Optimizer (GWO), or Salp Swarm Algorithm (SSA), to further evaluate optimization performance under more complex planning scenarios. Moreover, validating the approach on larger-scale and more complex distribution networks will help assess both the scalability and computational efficiency of the proposed optimization framework for practical distribution system planning.

In conclusion, this study demonstrates the effectiveness of the Coyote Optimization Algorithm for determining optimal PV placement and sizing in distribution networks using voltage-dependent, time-varying load models and measured photovoltaic generation data. The proposed framework provides a realistic and statistically validated evaluation environment for PV allocation studies, enabling fair comparison between optimization algorithms under practical operating conditions. The results confirm that COA achieves significant reductions in power losses, improves voltage performance, and exhibits statistically superior optimization performance compared with the benchmark methods. These findings contribute to the development of more effective photovoltaic planning strategies and support the continued integration of distributed renewable energy resources into future distribution networks.

Acknowledgements

Gratitude is extended to the Solar Research Institute (SRI), Universiti Teknologi MARA (UiTM), for supporting publication of this article.

References

[1] Daravath, R. and Bali, S. K., A Metaheuristic Approach for the Optimal Allocation of Distributed Energy Resources in a Distribution System. *Journal of Renewable Energy and Smart Grid Technology*. 20 (2025) 70-81, doi: https://doi.org/10.69650/rast.2025.261307.

[2] Bawazir, R. O. and Cetin, N. S., Comprehensive overview of optimizing PV-DG allocation in power system and solar energy resource potential assessments. *Energy Reports.* 6 (2020) 173-208, doi: https://doi.org/10.1016/j.egyr.2019.12.010.

[3] Nasef, A. F., Alqahtani, M. H. and Shaheen, A. M., Technical and optimization insights into PV penetration in power distribution systems-based wild horse algorithm: Real cases on Egyptian networks. *Results in Engineering*. 25 (2025) 104603, doi: https://doi.org/10.1016/j.rineng.2025.104603.

[4] Bendriss, B., Sayah, S. and Hamouda, A., A novel improved Frilled Lizard algorithm for solving the optimal planning problem of renewable energy sources within distribution grids under uncertainties. *Energy Conversion and Management.* 326 (2025) 119465, doi: https://doi.org/10.1016/j.enconman.2024.119465.

[5] Sidi, M. O., Mosbah, M. and Zine, R., Optimization of the Placement and Size of Photovoltaic Source. *Computers, Materials and Continua.* 74 (2022) 1855-1870, doi: https://doi.org/10.32604/cmc.2023.030032.

[6] Guzman, C. P., Bañol Arias, N., Franco, J. F., Rider, M. J. and Romero, R., Enhanced coordination strategy for an aggregator of distributed energy resources participating in the day-ahead reserve market. *Energies*. 13 (2020) 1965, doi: https://doi.org/10.3390/en13081965.

[7] Paliwal, P., Comprehensive analysis of distributed energy resource penetration and placement using probabilistic framework. *IET Renewable Power Generation.* 15 (2021) 794-808, doi: https://doi.org/10.1049/rpg2.12069.

[8] Funde, N. and Yoon, S.-G., Rank-based energy scheduling strategy of networked microgrids in distribution systems. *IET Generation, Transmission & Distribution.* 16 (2022) 84-98, doi: https://doi.org/10.1049/gtd2.12279.

[9] Dinh, B. H., Nguyen, T. T., Nguyen, T. T. and Pham, T. D., Optimal location and size of photovoltaic systems in high voltage transmission power networks. *Ain Shams Engineering Journal*. 12 (2021) 2839-2858, doi: https://doi.org/10.1016/j.asej.2020.12.015.

[10] Chang, G. W. and Chinh, N. C., Coyote Optimization Algorithm-Based Approach for Strategic Planning of Photovoltaic Distributed Generation. *IEEE Access.* 8 (2020) 36180-36190, doi: https://doi.org/10.1109/ACCESS.2020.2975107.

[11] Liu, N., Li, C., Chen, L. and Wang, J., Hybrid data-driven and model-based distribution network reconfiguration with lossless model reduction. *IEEE Transactions on Industrial Informatics*. 18 (2021) 2943-2954, doi: https://doi.org/10.1109/TII.2021.3103934.

[12] Yazdavar, A. H., Shaaban, M. F., El-Saadany, E. F., Salama, M. M. A. and Zeineldin, H. H., Optimal Planning of Distributed Generators and Shunt Capacitors in Isolated Microgrids With Nonlinear Loads. *IEEE Transactions on Sustainable Energy.* 11 (2020) 2732-2744, doi: https://doi.org/10.1109/TSTE.2020.2973086.

[13] Wang, C., Lei, S., Ju, P., Chen, C., Peng, C. and Hou, Y., MDP-based distribution network reconfiguration with renewable distributed generation: Approximate dynamic programming approach. *IEEE Transactions on Smart Grid*. 11 (2020) 3620-3631, doi: https://doi.org/10.1109/TSG.2019.2963696.

[14] Pareek, P., Yu, W. and Nguyen, H. D., Optimal Steady-State Voltage Control Using Gaussian Process Learning. *IEEE Transactions on Industrial Informatics.* 17 (2021) 7017-7027, doi: https://doi.org/10.1109/TII.2020.3047844.

[15] Harasis, S., Abdelgabir, H., Sozer, Y., Kisacikoglu, M. and Elrayyah, A., A center of mass determination for optimum placement of renewable energy sources in microgrids. *IEEE Transactions on Industry Applications.* 57 (2021) 5274-5284, doi: https://doi.org/10.1109/TIA.2021.3085674.

[16] Rafi, V., Dhal, P. K., Rajesh, M., Srinivasan, D. R., Chandrashekhar, M. and Reddy, N. M., Optimal placement of time-varying distributed generators by using crow search and black widow - Hybrid optimization. *Measurement: Sensors*. 30 (2023) 100900, doi: https://doi.org/10.1016/j.measen.2023.100900.

[17] Vempalle, R. and Dhal, P. K., Optimal analysis of time varying load radial distribution system with photovoltaic and wind generating system using novel hybrid optimization technique. *Renewable Energy Focus.* 41 (2022) 246-257, doi: https://doi.org/10.1016/j.ref.2022.03.004.

[18] Zhu, X., Wang, J., Yu, H., Ma, J., Li, J. and Li, C., A hierarchical time-varying optimization algorithm for Photovoltaic-energy storage to suppress three-phase imbalances in active distribution networks. *International Journal of Electrical Power & Energy Systems.* 167 (2025) 110608, doi: https://doi.org/10.1016/j.ijepes.2025.110608.

[19] Ahmed, A., Khan, M. F. N., Khan, I., Alquhayz, H., Khan, M. A. and Kiani, A. T., A Novel Framework to Determine the Impact of Time Varying Load Models on Wind DG Planning. *IEEE Access.* 9 (2021) 11342-11357, doi: https://doi.org/10.1109/ACCESS.2021.3050307.

[20] Ahmed, A., Nadeem, M. F., Kiani, A. T. and Khan, I. An overview on optimal planning of distributed generation in distribution system and key issues. in *2021 IEEE Texas Power and Energy Conference (TPEC).* (2021) 1-6, doi: https://doi.org/10.1109/TPEC51183.2021.9384976.

[21] Chaduvula, H. and Das, D., Investigating effect of various time varying load models in grid connected microgrid system integrated with renewables and cogeneration units. *International Journal of Ambient Energy*. 44 (2023) 2540-2552, doi: https://doi.org/10.1080/01430750.2023.2258130.

[22] Oda, E. S., Abd El Hamed, A. M., Ali, A., Elbaset, A. A., Abd El Sattar, M. and Ebeed, M., Stochastic optimal planning of distribution system considering integrated photovoltaic-based DG and DSTATCOM under uncertainties of loads and solar irradiance. *IEEE access.* 9 (2021) 26541-26555, doi: https://doi.org/10.1109/ACCESS.2021.3058589.

[23] Khasanov, M., Kamel, S., Awad, A. and Jurado, F., Optimal planning DG and BES units in distribution system consideringuncertainty of power generation and time-varying load. *Turkish Journal of Electrical Engineering and Computer Sciences.* 29 (2021) 773-795, doi: https://doi.org/10.3906/elk-2003-46.

[24] Elseify, M. A., SeyyedAbbasi, A., Domínguez-García, J. L. and Kamel, S., Probabilistic optimal planning of multiple photovoltaics and battery energy storage systems in distribution networks: A boosted equilibrium optimizer with time-variant load models. *Journal of Energy Storage.* 73 (2023) 108986, doi: https://doi.org/10.1016/j.est.2023.108986.

[25] Asif, R. M., Rehman, A. U., Alsharabi, N., Rabbani, S., Shakir, M., Malik, N., Rehman, S. U. and Khan, A. A., Optimal Locating and Sizing of DG in Radial Distribution System Using Modified Shuffled Frog Leaping Algorithm. *IETE Journal of Research.* 70 (2024) 2148-2165, doi: https://doi.org/10.1080/03772063.2022.2150690.

[26] Savio, F. M., Joshua, S. V., Usha, K., Faheem, M., Kannadasan, R. and Khan, A. A., Design of a solar-wind hybrid renewable energy system for power quality enhancement: a case study of 2.5 mw real time domestic grid. *Engineering Reports.* 7 (2025) e13101, doi: https://doi.org/10.1002/eng2.13101.

[27] Janamala, V. and Reddy, D. S., Coyote optimization algorithm for optimal allocation of interline–Photovoltaic battery storage system in islanded electrical distribution network considering EV load penetration. *Journal of Energy Storage.* 41 (2021) 102981, doi: https://doi.org/10.1016/j.est.2021.102981.

[28] Nguyen, T. T., Pham, T. D., Kien, L. C. and Van Dai, L., Improved Coyote Optimization Algorithm for Optimally Installing Solar Photovoltaic Distribution Generation Units in Radial Distribution Power Systems. *Complexity.* 2020 (2020) 1603802, doi: https://doi.org/10.1155/2020/1603802.

[29] Boukaroura, A., Slimani, L. and Bouktir, T., Optimal placement and sizing of multiple renewable distributed generation units considering load variations via dragonfly optimization algorithm. *Iranian Journal of Electrical and Electronic Engineering*. 16 (2020) 353, doi: https://doi.org/10.22068/IJEEE.16.3.353.

[30] Farhah, H., Abdullah, M. P. and Ali, A., IMPACT AND EVALUATION OF OPTIMIZED PV GENERATION IN THE DISTRIBUTION SYSTEM WITH VARYING LOAD DEMANDS. *Jurnal Teknologi* 85 (2023) 61-73, doi: 10.11113/jurnalteknologi.v85.18684.

[31] Isa, S. S. M., Ibrahim, M. N., Ahmad, A. M., Nordin, S., Dahlan, N. Y. and Jamahori, H. F. B. Optimizing Photovoltaic Systems for Power Losses Reduction under Time-Varying Loads: A Coyote Optimization Approach. in *2024 IEEE 14th International Conference on Control System, Computing and Engineering (ICCSCE).* 226-231, doi: https://doi.org/10.1109/ICCSCE61582.2024.10696590.

[32] Hanis Farhah Jamahori, M. P. A. A. A. A. A., Optimal Design and Performance Analysis of Multiple Photovoltaic with Grid-Connected Commercial Load. International Journal of Technology. 15 (2024) 291-319, doi: https://doi.org/10.14716/ijtech.v15i4.6019.

[33] Nor, N. M., Ali, A., Ibrahim, T. and Romlie, M. F. in *Sustainable Electrical Power Resources through Energy Optimization and Future Engineering: Planning of Distributed Renewable Energy Resources Using Genetic Algorithm.* (2018) 37-64, doi: https://doi.org/10.1007/978-981-13-0435-4_4.

[34] Pierezan, J. and Coelho, L. D. S. Coyote Optimization Algorithm: A New Metaheuristic for Global Optimization Problems. in *2018 IEEE Congress on Evolutionary Computation (CEC).* 1-8, doi: https://doi.org/10.1109/CEC.2018.8477769.

[35] Yuan, Z., Wang, W., Wang, H. and Yildizbasi, A., A new methodology for optimal location and sizing of battery energy storage system in distribution networks for loss reduction. *Journal of Energy Storage*. 29 (2020) 101368, doi: https://doi.org/10.1016/j.est.2020.101368.

[36] Zhu, J.-H., Wang, J.-S., Zhang, X.-Y., Song, H.-M. and Zhang, Z.-H., Mathematical distribution coyote optimization algorithm with crossover operator to solve optimal power flow problem of power system. *Alexandria Engineering Journal*. 69 (2023) 585-612, doi: https://doi.org/10.1016/j.aej.2023.02.023.

[37] Abdallah, E. M., Elsayed, M. I., Elgazzar, A. A. and Hassan, Amal A., Coyote multi-objective optimization algorithm for optimal location and sizing of renewable distributed generators. *International Journal of Electrical and Computer Engineering (IJECE).* 11 (2021) 975-983, doi: https://doi.org/10.11591/ijece.v11i2.pp975-983.

[38] Albadr, M. A., Tiun, S., Ayob, M. and Al-Dhief, F., Genetic Algorithm Based on Natural Selection Theory for Optimization Problems. Symmetry. 12 (2020) 1758, doi: https://doi.org/10.3390/sym12111758.